Transverse-ultrasonic-attenuation determination of the energy gap between the normal and superconducting states of zinc*

E. H. Breashears, C. R. Cleavelin, and B. J. Marshall
Department of Physics, Texas Tech University, Lubbock, Texas 79409
(Received 25 August 1975)

Transverse-ultrasonic-attenuation measurements have been conducted on a high-purity zinc single crystal in the normal and superconducting states for certain polarizations with propagation parallel to the [0001], [10$\bar{1}$0], and [11$\bar{2}$0] directions. The anisotropic superconducting energy gap, total electronic attenuation, and residual electronic attenuation have been determined as a function of frequency in the 10–100-MHz range for these orientations. This study was made to compare the results with those of previous longitudinal-ultrasonic-attenuation measurements by Cleavelin and Marshall which indicated the existence of a highly anisotropic energy gap dependent on the value of $ql \simeq 1$ in the same zinc crystal. The present results with greater interaction selectivity further indicate this same behavior.

I. INTRODUCTION

In a previous paper[1] the anisotropic energy gap of superconducting zinc was determined from experimental measurements of the attenuation of longitudinal ultrasonic waves propagating along three independent directions. Multiple gaps and frequency-dependent behavior of the energy gap were indicated for ultrasound propagating parallel to the [10$\bar{1}$0] and [11$\bar{2}$0] directions for $ql \simeq 1$, where $\vec{q}$ is the ultrasonic wave vector ($2\pi/\lambda$) and l is the electron mean-free-path.[1]

Leibowitz[2] has discussed the "effective zone" specifying which electrons on the Fermi surface will interact with a longitudinal or transverse ultrasonic wave. Utilizing the free-electron model and $ql \gtrsim 1$, the "effective zone" for either longitudinal or transverse waves can be determined from

$$\cos\theta \simeq v_s/v_F + 1/ql\,, \tag{1}$$

where θ indicates the angle between the Fermi velocity $\vec{v}_F$ and the sound velocity $\vec{v}_s$ parallel to $\vec{q}$. For large values of ql, the "effective zone" becomes a narrow band of electrons with Fermi velocities perpendicular to the direction of sound propagation ($\vec{q}$). In addition, Leibowitz[2] states that for transverse ultrasonic waves, the interaction is weighted toward the electrons on the "effective zone" having Fermi velocities parallel to the polarization vector ($\vec{\epsilon}$).

Thus, it became desirable to extend the previous longitudinal study[1] by determing the anisotropic energy gap from experimental measurements of the attenuation of transverse ultrasonic waves in the same zinc single crystal.

II. SAMPLE

The sample used in these measurements has been discussed previously.[1] It is a smaller crystal machined from a high-purity (99.9999%) zinc single crystal obtained from the Materials Research Corp.[3] The structure of crystalline zinc is hexagonal closed packed (hcp), allowing three independent directions to be chosen for study ([0001] or c axis, [10$\bar{1}$0], and [11$\bar{2}$0]). Since these three directions are mutually orthogonal, the sample was machined with an Elox TQH-31 electric-discharge machine into the form of a rectangular parallelpiped with approximate dimensions of $4.2 \times 5.8 \times 7.9$ mm^3, respectively. The sample was oriented along the desired axes using the Laue backreflection technique.[4]

The average electron mean free path (l) at impurity-limited temperatures (less than 4 K) has been estimated by the previous work[1] to be approximately 0.1 cm for the c axis, 0.003–0.006 cm for the [10$\bar{1}$0] axis, and 0.001–0.005 cm for the [11$\bar{2}$0] axis. These approximate values were obtained by two methods. First, by fitting the normal-state longitudinal ultrasonic attenuation data to the Pippard theory,[1] and secondly, by a method proposed by Deaton and Gavenda,[5] and previously used by Deaton[6] in a study of zinc and cadmium. This method is basically a magnetoacoustical analysis of the high magnetic field attenuation of longitudinal ultrasonic waves utilizing the free electron model. More discussion is given elsewhere.[1]

During the course of this study, a dependence of the transverse ultrasonic attenuation on the wave amplitude (amplitude dependence) was observed for propagation parallel to the c axis. Therefore, the sample was etched to clean its surface and then annealed to remove some of the dislocations which produced the amplitude dependence. The etching solution was 4% by volume of concentrated nitric acid in methanol. The sample was annealed under vacuum in a Thermolyne electric furnace type 10500 for 24 h at 340 °C. The new approximate dimensions of the sample were $3.9 \times 5.5 \times 7.5$ mm^3.

III. EXPERIMENTAL

The method used to obtain the transverse ultrasonic attenuation in the zinc sample was the standard single-ended transducer pulse-echo technique.[7] A block diagram of the complete continuously measuring ultrasonic system is shown in Fig. 1. This system makes use of phase-sensitive detection to increase the signal to noise ratio in the amplification of the echoes. This system was used to record the variation in height of a given echo as a voltage on the Y axis of the Moseley model No. 2D-2A X-Y recorder. A detailed discussion of the operation of the complete system is reported elsewhere.[1,8,9]

The stable low temperatures (below 1 K) were produced by a conventional ^{3}He evaporative refrigerator. The cryostat incorporated an rf transmission line for generating the ultrasonic waves. This refrigerator could reach and maintain a minimum temperature of about 0.37 K. This ^{3}He refrigerator cryostat is also discussed elsewhere.[1,9,10]

The primary temperature reference in this study was the ^{3}He vapor pressure as measured by a Wallace and Tiernan (W & T)model No. FA-160 absolute-pressure gauge. The range of 1.00–20.00 Torr was monitored. The temperature of the ^{3}He liquid and consequently the sample could be determined by finding the corresponding ^{3}He vapor pressure in the T_{62} ^{3}He thermometry tables prepared by Sherman, Sydoriak, and Roberts.[11] Two $\frac{1}{2}$-W Allen Bradley carbon-resistance thermometers (CRT) with nominal room-temperature resistances of 2.7 and 5.1 Ω were employed as secondary thermometers. The resistance was determined by the four-terminal measuring method, using a constant current of 1.000 μA as shown in Fig. 1. The constant current through the CRT's was set by reading the voltage drop across a 0.05% standard resistor (SR) in a series with the CRT's as shown in Fig. 1. The system recorded temperature variation (resistance) on the X axis of the X-Y recorder. The CRT's were calibrated directly against the W & T pressure gauge. A least-squares fit of these data to the Clement Quinnell equation[12] was used to extend each calibration to lower temperatures. Transverse or "Y-cut" piezoelectric quartz transducers vibrating at a fundamental frequency of 10 MHz, or an odd harmonic of this frequency were used to generate the transverse ultrasonic waves. The transducer was bonded to the sample face with a thin layer of Dow Corning DC-11 silicon grease.

It was desired to eliminate the effects of the earth's magnetic field on the sample.[13] This was accomplished by constructing two sets of constant current-carrying coils around the outer Dewar, so as to individually cancel the vertical and horizontal components of the earth's magnetic field.

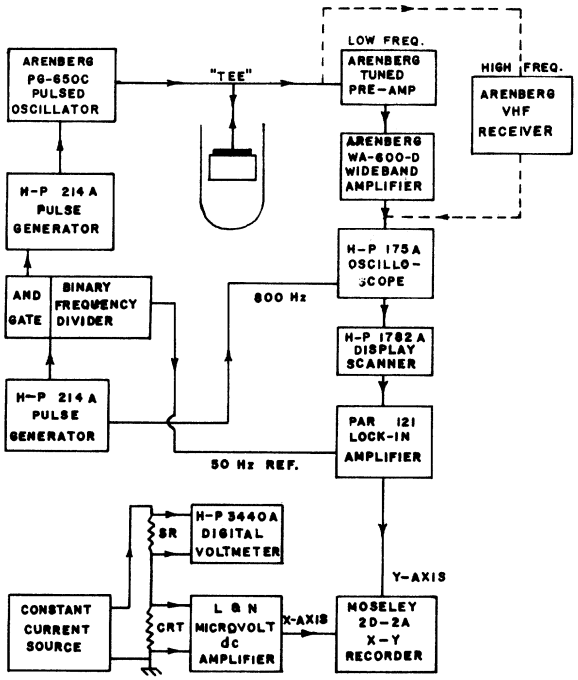

FIG. 1. Block diagram of the ultrasonic attenuation and temperature measurement systems.

IV. ANALYSIS OF DATA

A. Transverse ultrasonic attenuation in normal metals

Pippard[14] has developed an expression for the impurity-limited electronic attenuation (α_n) of transverse ultrasonic waves in normal metals. These metals are considered to be isotropic and to conform to the free-electron model with a well-defined relaxation time (τ). The expression is

$$\alpha_n = \frac{Nm}{\rho v_s' \tau}\left(\frac{1-g}{g}\right), \tag{2}$$

where

$$g = \frac{3}{2(ql)^2}\left(\frac{(ql)^2+1}{ql}\tan^{-1}(ql) - 1\right), \tag{3}$$

N is the number of electrons per unit volume, m is the effective electron mass, ρ is the density, and v_s' is the transverse wave velocity.

If $ql \geq 1$ and the frequency of the wave is less than about 10^9 Hz, the expression reduces to

$$\alpha_n \simeq \frac{4}{3}\frac{Nmv_F}{\rho v_s'^2}\omega. \tag{4}$$

For this case, α_n should be proportional to the frequency, and independent of the value of ql. If

$ql \simeq 1$, Eq. (2) with Eq. (3) must be used to give the frequency dependence.

Since these expressions were developed for an isotropic metal, they should be modified for a real anisotropic normal metal. This has been discussed by Morse,[15] and again by Pippard.[16]

B. Transverse ultrasonic attenuation in superconductors

Some experimental observations[2,13,17,18] of the behavior of the attenuation of transverse ultrasonic waves as a function of temperature in superconductors with $ql \geq 1$ have indicated two distinct regions. The first, characterized by a sharp decrease with temperature near T_c (superconducting transition temperature), is called the "rapid-fall" region. It is thought to be an electromagnetic attenuation contribution, and is denoted by α_E. The second, characterized by a more gradual decrease with temperature, is called the "residual" attenuation region. It is denoted by α_R.

The Bardeen, Cooper, and Schrieffer[19] (hereafter BCS) theory of superconductivity predicts that the ratio of superconducting to normal electronic attenuation for low-frequency longitudinal ultrasonic waves when $ql > 1$ is given by

$$\frac{\alpha_s}{\alpha_n} = \frac{2}{e^{\Delta(T)/kT}+1} = 2f(\Delta(T)), \tag{5}$$

where k is Boltzmann's constant, T is the absolute temperature, f is the Fermi function, and $\Delta(T)$ is the BCS temperature-dependent energy gap. The value of $\Delta(T)$ varies from 0 at T_c to a maximum value $1.76kT_c$ at absolute zero for isotropic superconductors. $\Delta(T)$ is a measure of the energy required per electron to completely disassociate a Cooper pair.[20] For a real anisotropic superconductor, the value of $\Delta(0)$ may vary with crystallographic direction, and depart from the BCS result of $1.76kT_c$. This can be expressed by $\Delta(\vec{q}, 0)$, where the phonon wave vector $(\vec{q})$ indicates propagation parallel to that direction.

Tsuneto[21] has shown that Eq. (5) correctly describes the "residual" region of transverse ultrasonic waves for impurity-limited attenuation. In order to make the determination of $\Delta(\vec{q}, 0)$ more convenient, Eq. (5) can be rewritten as

$$\ln\left(2\frac{\alpha_n}{\alpha_s}-1\right) = \frac{\Delta(\vec{q}, 0)}{kT_c}\frac{G(t)}{t}, \tag{6}$$

where $G(t) = \Delta(T)/\Delta(0)$ for an ideal superconductor, and $t = T/T_c$ is the reduced temperature. The function $G(t)$ has been tabulated from the BCS theory by Mühlschlegel.[22] It has been found to be more convenient to use the analytical expression developed by Clem,[23]

$$G(t) = 1.7367(1-t)^{1/2}[1 - 0.4095(1-t) - 0.0626(1-t)^2]. \tag{7}$$

This form has been shown to reproduce Mühlschlegel's values for $G(t)$, with an error of less than 0.1% for $t > 0.4$.

As can be observed from Eq. (6), a plot of $\ln(2\alpha_n/\alpha_s - 1)$ vs $G(t)/t$ should yield a straight line with a slope of $\Delta(\vec{q}, 0)$ expressed in units of kT_c. Also, the straight line should pass through the origin, that is, the point (0, 0). If multiple energy gaps do exist, they should appear as different slopes in this plot.

Figure 2 is representative of the voltage data reproduced from the X-Y recorder. In order to analyze this data, the "rapid-fall" (if present) and the "residual" attenuation regions must be separated. This can be done by defining a voltage in the superconducting state at the transition temperature, $V_s(T_c)$, as shown in Fig. 2. The ratio of superconducting to normal-state electronic attenuation of a given echo for the "residual" region is given by

$$\frac{\alpha_s}{\alpha_n} = \frac{\log_{10}[V_s(0)/V_s(T)]}{\log_{10}[V_s(0)/V_s(T_c)]}. \tag{8}$$

The "residual" attenuation in dB/cm is given by

$$\alpha_R = \frac{20}{2n'L}\log_{10}\left(\frac{V_s(0)}{V_s(T_c)}\right), \tag{9}$$

where n' is the echo number and L is the sample length in cm. In the same manner, the total electronic attenuation is defined as

$$\alpha_n = \frac{20}{2n'L}\log_{10}\left(\frac{V_s(0)}{V_n(T_c)}\right). \tag{10}$$

It should be noted that the electromagnetic attenuation contribution is given by

$$\alpha_E = \alpha_n - \alpha_R. \tag{11}$$

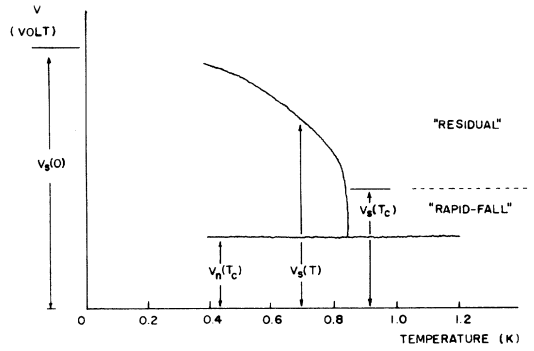

FIG. 2. Representation of the transverse voltage data vs temperature, as reproduced from the X-Y recorder with $ql \geq 1$.

However, Eqs. (8)–(10) cannot be determined unless the values of $V_s(0)$ and $V_s(T_c)$ are known for each experimental curve. To overcome this problem, a program for the IBM VS/370 computer was used to analyze the data. The value of $V_s(0)$ was varied to minimize the standard deviation of a least-squares fit to $\ln(2\alpha_n/\alpha_s - 1)$ vs $G(t)/t$ with $V_s(T_c) = V_n(T_c)$. This would yield a straight line with a large positive value for the $\ln(2\alpha_n/\alpha_s - 1)$ intercept. The value of $V_s(T_c)$ was increased, and a new $V_s(0)$ was determined. This process was repeated until values of $V_s(0)$ and $V_s(T_c)$ were found to give a $\ln(2\alpha_n/\alpha_s - 1)$ intercept of approximately zero, and a minimum standard deviation for the least-squares fit to Eq. (6). The slope or $\Delta(\vec{q}, 0)$ could then be found. If more than one slope is found to occur, the $V_s(0)$ is determined from the slope occurring at the lower reduced temperatures. This slope then corresponds to $\Delta(\vec{q}, 0)$. The slope at the higher reduced temperatures, called $\Delta^*(\vec{q}, 0)$, is calculated from the same $V_s(0)$.

It should be noted that this technique does not uniquely determine the functional form of $\alpha_s(T)$, although it does provide experimental verification for the consistency of the experimental observations with the BCS relation, Eq. (5). Another functional form has been observed for longitudinal ultrasonic waves in several elemental superconductors investigated in this laboratory. It is given by

$$\alpha_s/\alpha_n \propto t^3. \tag{12}$$

These data can be found in Fig. 2 of Ref. 1. In the present work, it has also been observed that transverse ultrasonic attenuation data fit this same functional form.

Some amplitude dependence was observed in this study, especially for propagation parallel to the c axis. This was minimized by the process of annealing and by keeping the ultrasonic wave amplitude as low as possible. The largest measured voltage (peak to peak) applied to the transducer was never greater than 10 V.

V. RESULTS

A. Value of T_c

The critical or superconducting transition temperature (T_c) was found to be 0.840 ± 0.005 K, independent of propagation direction. It was also found that there was essentially no difference in the value of T_c, or in the shape of the "rapid-fall" attenuation region between data taken with and without the elimination of the effects of the earth's magnetic field on the sample.

B. Results for $\vec{q} \parallel [0001]$ and $\vec{\epsilon} \parallel [10\bar{1}0]$

Representative plots of $\ln(2\alpha_n/\alpha_s - 1)$ vs $G(t)/t$ at the indicated frequencies for $\vec{q} \parallel [0001]$ and $\vec{\epsilon} \parallel [10\bar{1}0]$ are shown in Fig. 3. It was observed that the plots could be fit with one slope over the entire temperature range for each frequency. The values of $\Delta(\vec{q}, 0)$, α_n and α_R are tabulated for this and other orientations in Table I, for each of the frequencies. The stated error shown with each value of $\Delta(\vec{q}, 0)$ has been estimated from the scatter between the values obtained from all plots of $\ln(2\alpha_n/\alpha_s - 1)$ vs $G(t)/t$ at a given frequency. The error associated with α_n and α_R has been estimated in the same manner to be about ±1.00 dB/cm. This large error comes about in the computer extrapolation to determine $V_s(0)$ and $V_s(T_c)$, and does not represent the sensitivity of the attenuation measurement system for any given measurement. The system has an approximate accuracy of 0.1 dB/cm, with a resolution of 0.01 dB/cm.

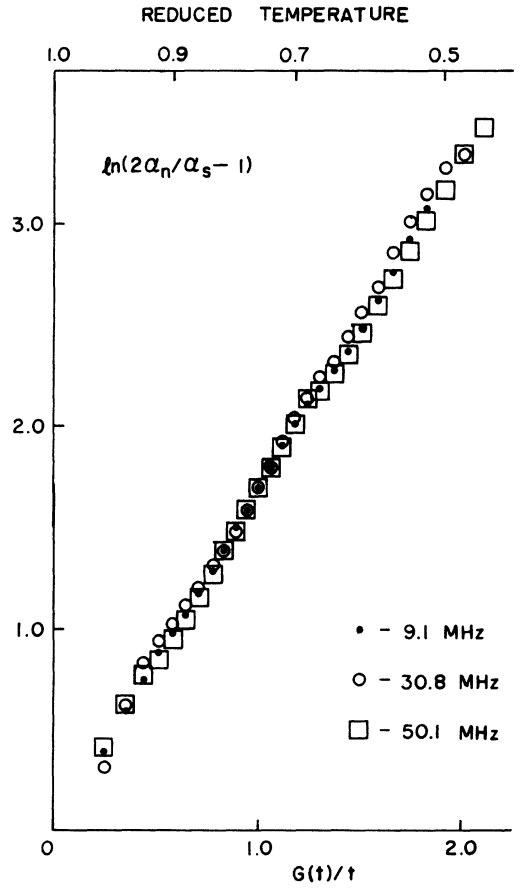

FIG. 3. Representations of $\ln(2\,\alpha_n/\alpha_s - 1)$ vs $G(t)/t$ at frequencies of 9.1, 30.8, and 50.1 MHz for $\vec{q} \,||\, [0001]$ and $\vec{\epsilon} \,||\, [10\bar{1}0]$.

TABLE I. Superconducting energy gap $\Delta(\vec{q},0)$, apparent second gap $\Delta^*(\vec{q},0)$, total electronic attenuation α_n, and residual electronic attenuation α_R as a function of frequency and direction.

Frequency (MHz)	α_n (dB/cm)	α_R (dB/cm)	$\Delta^*(\vec{q},0)$ (kT_C)	$\Delta(\vec{q},0)$ (kT_C)
		$\vec{q}\,\|\|\,[0001]$ and $\vec{\epsilon}\,\|\|\,[10\bar{1}0]$		
9.1	2.7	2.1	...	1.64 ± 0.20
30.8	5.0	3.2	...	1.66 ± 0.20
50.1	6.6	4.4	...	1.64 ± 0.20
		$\vec{q}\,\|\|\,[0001]$ and $\vec{\epsilon}\,\|\|\,[10\bar{1}0]$ annealed		
10.1	2.4	1.8	...	1.46 ± 0.15
30.7	4.6	3.3	...	1.59 ± 0.15
48.5	7.4	6.1	...	1.51 ± 0.15
		$\vec{q}\,\|\|\,[0001]$ and $\vec{\epsilon}\,\|\|\,[11\bar{2}0]$ annealed		
10.8	3.0	2.5	...	1.50 ± 0.20
29.8	6.6	5.2	...	1.50 ± 0.10
48.0	8.6	6.2	...	1.51 ± 0.20
		$\vec{q}\,\|\|\,[10\bar{1}0]$ and $\vec{\epsilon}\,\|\|\,[11\bar{2}0]$		
10.7	1.4	1.2	1.68 ± 0.10	1.42 ± 0.20
30.6	4.2	3.3	...	1.52 ± 0.15
50.0	5.6	4.3	...	1.63 ± 0.15
		$\vec{q}\,\|\|\,[11\bar{2}0]$ and $\vec{\epsilon}\,\|\|\,[0001]$		
10.7	2.0	1.3	2.11 ± 0.20	1.45 ± 0.20
30.0	2.3	2.3	...	1.57 ± 0.20
49.5	2.5	2.3	...	1.52 ± 0.20
70.0	2.4	1.3	...	1.65 ± 0.20
89.2	4.3	3.5	2.26 ± 0.20	1.75 ± 0.20

C. Results for $\vec{q}\,\|\|\,[0001]$ and $\vec{\epsilon}\,\|\|\,[10\bar{1}0]$ annealed

Representative plots of $\ln(2\alpha_n/\alpha_s - 1)$ vs $G(t)/t$ at the indicated frequencies for $\vec{q}\,\|\|\,[0001]$ and $\vec{\epsilon}\,\|\|\,[10\bar{1}0]$ with the annealed zinc sample are shown in Fig. 4. It was found that the plots indicated one value of $\Delta(\vec{q},0)$ for each frequency. The total electronic attenuation (α_n) was found to vary linearly with frequency. The electromagnetic attenuation (α_E) increased with frequency. It was observed that the annealing process lowered the energy gap by approximately $0.15kT_c$ for each frequency.

D. Results for $\vec{q}\,\|\|\,[0001]$ and $\vec{\epsilon}\,\|\|\,[11\bar{2}0]$ annealed

Representative plots of $\ln(2\alpha_n/\alpha_s - 1)$ vs $G(t)/t$ at the indicated frequencies for $\vec{q}\,\|\|\,[0001]$ and $\vec{\epsilon}\,\|\|\,[11\bar{2}0]$ with the annealed zinc samples are shown in Fig. 5. Only one value of $\Delta(\vec{q},0)$ was indicated for each frequency. α_n was found to vary approximately linearly with frequency, with α_E increasing with frequency.

E. Results for $\vec{q}\,\|\|\,[10\bar{1}0]$ and $\vec{\epsilon}\,\|\|\,[11\bar{2}0]$

Representative plots of $\ln(2\alpha_n/\alpha_s - 1)$ vs $G(t)/t$ at the indicated frequencies for $\vec{q}\,\|\|\,[10\bar{1}0]$ and $\vec{\epsilon}\,\|\|\,[11\bar{2}0]$ are shown in Fig. 6. It was found that the data for 10.7 MHz indicated two different slopes. The value $\Delta^*(\vec{q},0)$ was found to occur in the higher-temperature range from $0.98 > t > 0.80$. A smaller slope $\Delta(\vec{q},0)$ was found for $t < 0.80$. $\Delta^*(\vec{q},0)$ tended to the value of $\Delta(\vec{q},0)$ as the frequency was increased above 10.7 MHz. The slopes at 30.6 and 50.0 MHz are each represented by only one value of $\Delta(\vec{q},0)$. The value of $\Delta(\vec{q},0)$ increased slightly with frequency, while α_n varies linearly with frequency and α_E increases with frequency.

F. Results for $\vec{q}\,\|\|\,[11\bar{2}0]$ and $\vec{\epsilon}\,\|\|\,[0001]$

Representative plots of $\ln(2\alpha_n/\alpha_s - 1)$ vs $G(t)/t$ at the indicated frequencies for $\vec{q}\,\|\|\,[11\bar{2}0]$ and $\vec{\epsilon}\,\|\|\,[0001]$ are shown in Fig. 7. The best fit for the data at 10.7 and 89.2 MHz required two energy gaps. $\Delta^*(\vec{q},0)$ was found to occur at higher re-

duced temperatures in the range of $0.98 > t > 0.88$ for both frequencies. The lower value of $\Delta(\vec{q}, 0)$ was found to occur for $t < 0.88$. The plots at other frequencies were found to require one value of $\Delta(\vec{q}, 0)$ over the entire temperature range. The values of $\Delta(\vec{q}, 0)$ were found to increase with frequency.

The frequency dependence of α_n in the study of this orientation was found to be unlike that theoretically expressed by Eq. (2) with Eq. (3) for $ql \simeq 1$. Based on the previous longitudinal data for $\vec{q} \| [11\bar{2}0]$[1], a portion of the "hump" was indicated. More importantly, the value of α_E does not necessarily increase with frequency. The data taken at 30.0 MHz does not show a "rapid-fall" region of attenuation, whereas the data for 10.7 MHz does.

G. Other orientations

Energy gaps were not determined for the other orientations. Some information for $\vec{q} \| [10\bar{1}0]$ and $\vec{\epsilon} \| [0001]$ can be found elsewhere.[18] Values of the electronic attenuation and energy gaps for $\vec{q} \| [11\bar{2}0]$ and $\vec{\epsilon} \| [10\bar{1}0]$, as well as for $\vec{q} \| [10\bar{1}0]$ and $\vec{\epsilon} \| [11\bar{2}0]$ can also be found elsewhere.[24]

VI. CONCLUSIONS

Electronic thermal-conductivity measurements conducted by Zavaritskii[25] have indicated a maximum energy gap of about $1.75kT_c$ parallel to the c axis and a minimum of $1.20kT_c$ perpendicular to the c axis in superconducting zinc. Microwave absorption measurements by Evans *et al.*[26] have shown that an average energy gap of about $1.5kT_c$ is associated with most of the Fermi surface of zinc. However, a small part can be associated with an average energy gap of about $2.0kT_c$ near the c axis. Other nonultrasonic measurements[27-29] have indicated an anisotropy consistent with the above values.

Several longitudinal attenuation measurements

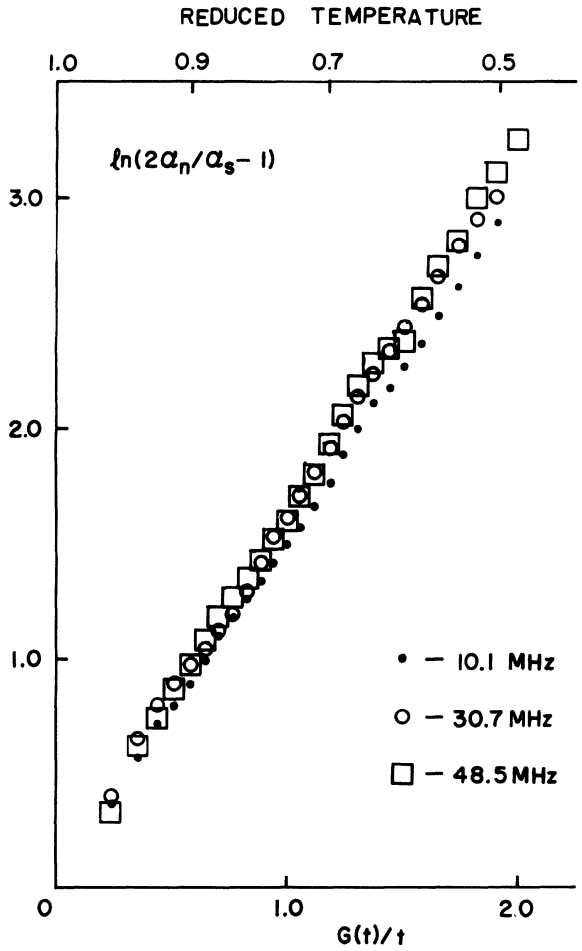

FIG. 4. Representations of $\ln(2\,\alpha_n/\alpha_s - 1)$ vs $G(t)/t$ at frequencies of 10.1, 30.7, and 48.5 MHz for $\vec{q} \| [0001]$ and $\vec{\epsilon} \| [10\bar{1}0]$, with the annealed sample.

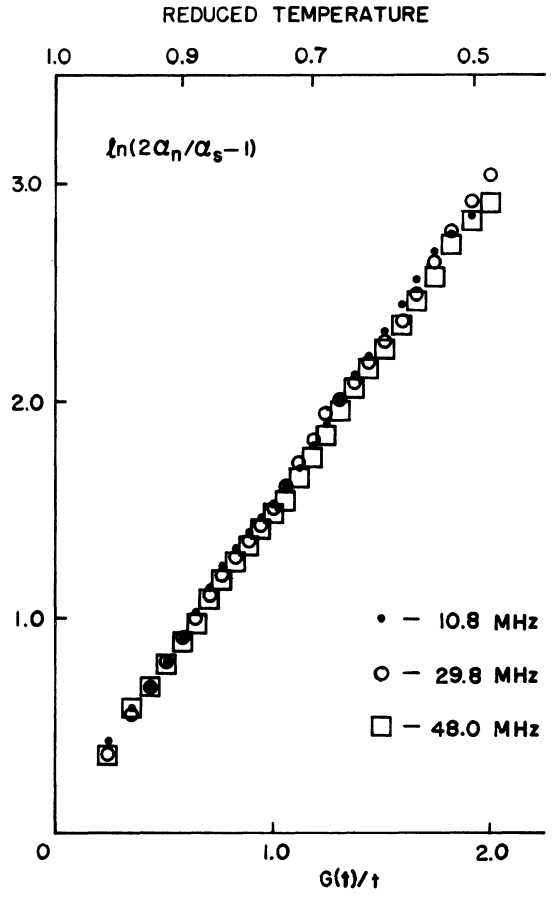

FIG. 5. Representations of $\ln(2\,\alpha_n/\alpha_s - 1)$ vs $G(t)/t$ at frequencies of 10.8, 29.8, and 48.0 MHz for $\vec{q} \| [0001]$ and $\vec{\epsilon} \| [11\bar{2}0]$ with the annealed sample.

of the energy gap of superconducting zinc have been made. Dobbs *et al.*[30] have found values of 1.71, 1.90, and 1.82 in units of kT_c for $\vec{q} \| [0001]$, $\vec{q} \| [10\bar{1}0]$, and $\vec{q} \| [11\bar{2}0]$, respectively. Bohm and Horwitz[31] have found values of $1.70kT_c$ and $1.90kT_c$ for $\vec{q} \| [10\bar{1}0]$ and $\vec{q} \| [11\bar{2}0]$, respectively. Work conducted by Goncz and Neighbors (refer to Ref. 1) indicates an energy gap of about $1.60kT_c$ for $\vec{q} \| [0001]$. Cleavelin and Marshall[1] (refer to Table II) have previously measured the limiting energy gaps of this zinc sample to be 1.50, 1.41, and 1.90 in units of kT_c for $\vec{q} \| [0001]$, $\vec{q} \| [10\bar{1}0]$, and $\vec{q} \| [11\bar{2}0]$, respectively. Lou and Bömmel[18] have recently obtained an energy gap of approximately $1.50kT_c$ for either longitudinal waves with $\vec{q} \| [0001]$ and $\vec{q} \| [10\bar{1}0]$, or for transverse waves with $\vec{q} \| [10\bar{1}0]$ and $\vec{\epsilon} \| [0001]$. The measurements were made on their zinc sample with the smallest concentration of impurities. More recently, Almond *et al.*[24] have found energy gaps of $1.60kT_c$ for $\vec{q} \| [10\bar{1}0]$ and $\vec{\epsilon} \| [11\bar{2}0]$ and $1.55kT_c$ for $\vec{q} \| [11\bar{2}0]$ and $\vec{\epsilon} \| [10\bar{1}0]$.

The complex Fermi surface of zinc as presented by Gibbons and Falicov[32] is composed of first and second bands of holes (caps and monster) with third and fourth bands of electrons (lens centered on Γ and needles centered on K). The third and fourth bands of electrons centered on L (butterflies and cigars) are raised above the Fermi level and are void of electrons.[33] The lens appears to be nearly free electron like. A comparison based on the interaction "selectivity" as given by Leibowitz[2] can now be made between the previous longitudinal[1] and these transverse measurements of the energy gaps of this zinc sample.

The "effective zone" for $\vec{q} \| [0001]$ should be a narrow band perpendicular to the c axis since $ql \gg 1$. The weighting of the interaction toward any particular part of this band should not change the value of the energy gap. This was found to be true using the annealed data for $\vec{q} \| [0001]$.

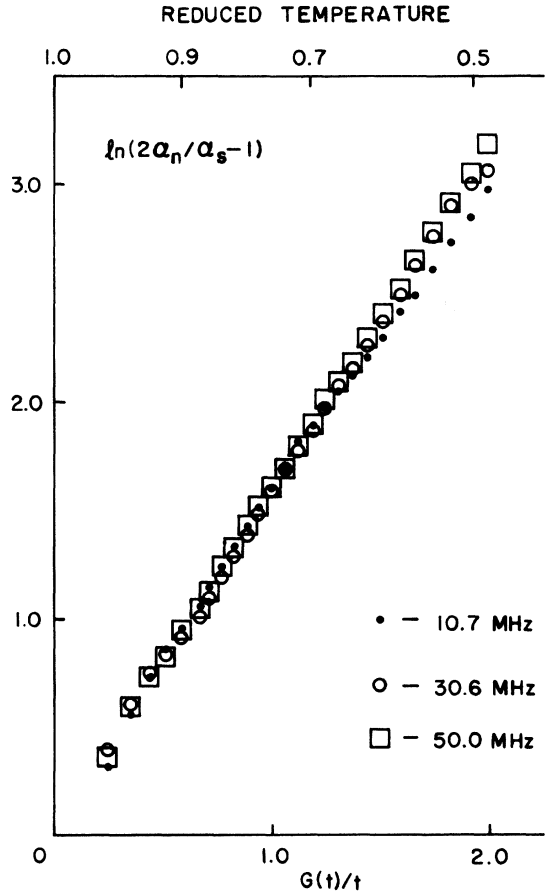

FIG. 6. Representation of $\ln(2\,\alpha_n/\alpha_s - 1)$ vs $G(t)/t$ at frequencies of 10.7, 30.6, and 50.0 MHz for $\vec{q} \,||\, [10\bar{1}0]$ and $\vec{\epsilon} \,||\, [11\bar{2}0]$.

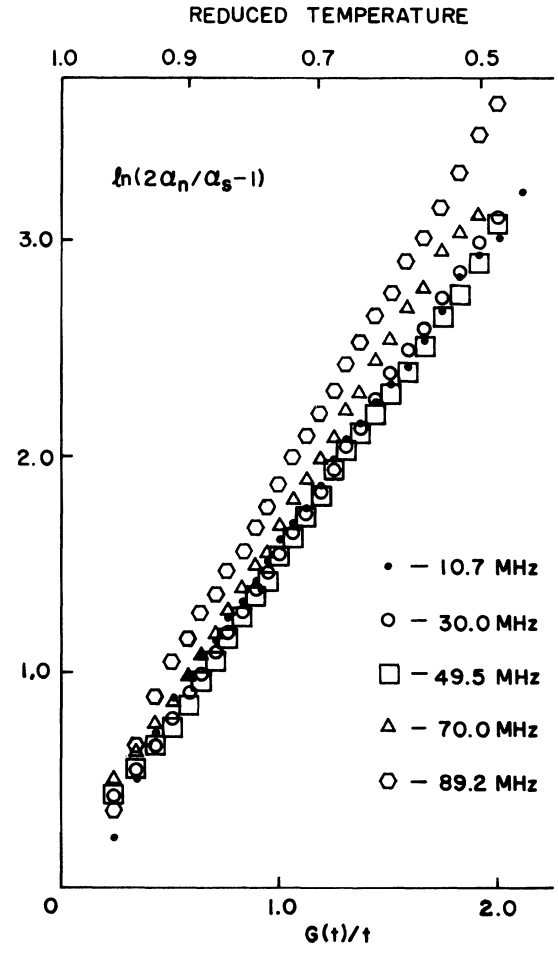

FIG. 7. Representations of $\ln(2\,\alpha_n/\alpha_s - 1)$ vs $G(t)/t$ at frequencies of 10.7, 30.0, 49.5, 70.0, and 89.2 MHz for $\vec{q} \,||\, [11\bar{2}0]$ and $\vec{\epsilon} \,||\, [0001]$.

TABLE II. Effective energy gap $2\Delta(\vec{q},0)$, and apparent second gap $2\Delta^*(\vec{q},0)$, in units of kT_C as a function of frequency and direction. Also given are the total electronic attenuation α_e in units of dB/cm, and the average ql value at each frequency studied (Ref. 1).

Average ql	Frequency (MHz)	α_e (dB/cm)	$2\Delta^*(\vec{q},0)$ (kT_C)	$2\Delta(\vec{q},0)$ (kT_C)
		$\vec{q}\parallel[0001]$		
180	9.0	4.5	•••	3.00 ±0.10
650	32.0	19.8	•••	3.00 ±0.10
1010	50.3	33.0	•••	3.02 ±0.10
		$\vec{q}\parallel[10\bar{1}0]$		
0.39	9.0	0.3	2.48 ±0.20	2.74 ±0.10
1.15	31.5	1.8	•••	2.78 ±0.10
1.92	51.1	3.9	•••	2.94 ±0.20
2.69	70.6	6.4	•••	2.82 ±0.10
		$\vec{q}\parallel[11\bar{2}0]$		
0.13	9.4	0.6	3.58 ±0.20	2.96 ±0.10
0.38	31.5	0.2	•••	3.20 ±0.10
0.64	53.0	4.4	4.66 ±0.20	3.52 ±0.10
0.90	70.6	6.5	4.80 ±0.20	3.98 ±0.10
1.15	90.5	7.3	5.00 ±0.20	4.02 ±0.20
1.41	110	6.9	4.42 ±0.20	3.96 ±0.20
1.67	130	6.2	•••	3.76 ±0.10
1.92	150	7.5	•••	3.74 ±0.10
2.18	170	9.2	•••	3.80 ±0.10

The "effective zone" for $\vec{q}\parallel[10\bar{1}0]$ should be a wide band perpendicular to the $[10\bar{1}0]$ direction, since $ql \gtrsim 1$. This band contains electrons represented by small energy gaps and a weighting of the interaction toward either the [0001][18] or $[11\bar{2}0]$[24] direction should give the minimum value. The "effective zone" for $\vec{q}\parallel[11\bar{2}0]$ should be a wide band perpendicular to the $[11\bar{2}0]$ direction since $ql \gtrsim 1$. This band contains electrons represented by small energy gaps perpendicular to the c axis, as well as electrons represented by large energy gaps parallel to the c axis. A weighting of the interaction toward the $[10\bar{1}0]$ direction[24] should yield low values of the energy gaps, while a weighting toward the [0001] direction should yield higher values for the energy gaps. The energy gaps determined in this study and tabulated in Table I do show these effects.

The assignment of multiple energy gaps for transverse ultrasonic attenuation measurements is at most tentative, since the average apparent gap over the "effective zone" at the higher reduced temperatures approaches the value of the average gap at the lower reduced temperatures as all parts of the "effective zone" approach $ql > 1$. This most likely indicates that the appearance of multiple gaps in the data analysis, and the dependence of the gaps on ql in zinc probably arise due to anisotropy associated with each piece of the Fermi surface studied, and not to multiple energy surfaces found in higher Brillouin zones. Thus, as the transverse sound wave becomes more selective and interacts with a smaller portion of the Fermi surface, the average gap associated with the portion or "effective zone" becomes less anisotropic. This being due to the "effective zone" becoming a very narrow band as indicated by Eq. (1), as all parts of the "effective zone" approach $ql > 1$. Thus, some limiting average value of the energy gap will be obtained which depends on the "effective zone" and the weighting on the "effective zone," due to the polarization of the transverse sound wave. This is the type of behavior observed in the experimental data.

All plots of the total electronic attenuation versus frequency, except $\vec{q}\parallel[11\bar{2}0]$ and $\vec{\epsilon}\parallel[0001]$, were found to fit the functional form given by Pippard within the indicated error. The plot for $\vec{q}\parallel[11\bar{2}0]$ and $\vec{\epsilon}\parallel[0001]$ was believed to be a portion of the "hump," as observed by Cleavelin and Marshall.[1] Claiborne and Morse[13] have indicated that α_E should increase with frequency. This was

found to be true for all the data except $\vec{q} \| [11\bar{2}0]$ and $\vec{\epsilon} \| [0001]$. The anomalous absence of a "rapid-fall" region of attenuation at 30.0 MHz, while one did exist at 10.7 MHz, warrants further investigation.

ACKNOWLEDGMENT

The authors appreciate the assistance of Dr. W. O. Milligan, Director of Research for the Robert A. Welch Foundation.

*Work supported by the Robert A. Welch Foundation.
[1]C. R. Cleavelin and B. J. Marshall, Phys. Rev. B 10, 1902 (1974).
[2]J. R. Leibowitz, Phys. Rev. 133, A84 (1964).
[3]Materials Research Corp., Orangeburg, N.Y.
[4]B. D. Cullity, *Elements of X-Ray Diffraction* (Addison-Wesley, Reading, Mass., 1957).
[5]B. C. Deaton and J. D. Gavenda, Phys. Rev. 129, 1990 (1963).
[6]B. C. Deaton, Phys. Rev. 140, A2051 (1965).
[7]R. Truell, C. Elbaum, and B. Chick, *Ultrasonic Methods in Solid State Physics* (Academic, New York, 1969), pp. 53–70.
[8]R. B. Hemphill, Rev. Sci. Instrum. 39, 910 (1968).
[9]S. G. O'Hara and B. J. Marshall, Phys. Rev. B 8, 4175 (1973).
[10]R. A. Robbins and B. J. Marshall, J. Appl. Phys. 42, 2562 (1971).
[11]R. H. Sherman, S. G. Sydoriak, and T. R. Roberts, J. Res. Natl. Bur. Stand. (U.S.) 68, 579 (1964).
[12]J. R. Clement and E. H. Quinnell, Rev. Sci. Instrum. 23, 213 (1952).
[13]L. T. Claiborne and R. W. Morse, Phys. Rev. 136, A893 (1964).
[14]A. B. Pippard, Philos. Mag. 46, 1104 (1955).
[15]R. W. Morse, Prog. Cryog. 1, 221 (1959).
[16]A. B. Pippard, Proc. R. Soc. A 257, 165 (1960).
[17]K. Fossheim, Phys. Rev. Lett. 19, 81 (1967).
[18]D. Y. Lou and H. E. Bömmel, Phys. Rev. B 9, 3739 (1974).
[19]J. Bardeen, L. N. Cooper, and J. R. Schrieffer, Phys. Rev. 108, 1175 (1957).
[20]L. N. Cooper, Phys. Rev. 104, 1189 (1956).
[21]T. Tsuneto, Phys. Rev. 121, 402 (1961).
[22]B. Mühlschlegel, Z. Phys. 155, 313 (1959).
[23]J. R. Clem, Ann. Phys. (N.Y.) 40, 268 (1966).
[24]D. P. Almond, M. J. Lea, and E. R. Dobbs, Proc. R. Soc. A 343, 537 (1975).
[25]N. V. Zavaritskii, Zh. Eksp. Teor. Fiz. 39, 1193 (1960) [Sov. Phys.–JETP 12, 831 (1961)].
[26]J. B. Evans, M. P. Garfunkel, and D. A. Hayes, Phys. Rev. B 1, 3629 (1970).
[27]H. A. Boorse, Phys. Rev. Lett. 2, 391 (1959).
[28]E. Ducla-Soares and J. D. N. Cheeke, in *Proceedings of the Twelfth International Conference on Low Temperature Physics*, edited by E. Kanda (Academic Press of Japan, Tokyo, 1970), p. 305.
[29]D. Farrell, J. G. Parks, and B. R. Coles, Phys. Rev. Lett. 13, 328 (1964).
[30]E. R. Dobbs, M. J. Lea, and D. R. Peck, Proc. R. Soc. A 334, 379 (1973).
[31]H. V. Bohm and N. H. Horwitz, in *Proceedings of the Eighth International Conference on Low Temperature Physics* (Butterworths, London, 1963), p. 191.
[32]D. G. Gibbons and L. M. Falicov, Philos. Mag. 8, 177 (1963).
[33]R. W. Stark and L. M. Falicov, Phys. Rev. Lett. 19, 795 (1967).